

Breaking NoC Anonymity using Flow Correlation Attack

Hansika Weerasena, *Member, IEEE*, Pan Zhixin, *Member, IEEE*, Khushboo Rani, *Member, IEEE*,
and Prabhat Mishra, *Fellow, IEEE*

Abstract—Network-on-Chip (NoC) is widely used as the internal communication fabric in today’s multicore System-on-Chip (SoC) designs. Security of the on-chip communication is crucial because exploiting any vulnerability in shared NoC would be a goldmine for an attacker. NoC security relies on effective countermeasures against diverse attacks. We investigate the security strength of existing anonymous routing protocols in NoC architectures. Specifically, this paper makes two important contributions. We show that the existing anonymous routing is vulnerable to machine learning (ML) based flow correlation attacks on NoCs. We propose a lightweight anonymous routing that use traffic obfuscation techniques which can defend against ML-based flow correlation attacks. Experimental studies using both real and synthetic traffic reveal that our proposed attack is successful against state-of-the-art anonymous routing in NoC architectures with a high accuracy (up to 99%) for diverse traffic patterns, while our lightweight countermeasure can defend against ML-based attacks with minor hardware and performance overhead.

Index Terms—On-Chip Communication, Network-on-Chip Security, Anonymous Routing, Flow Correlation, Machine Learning

I. INTRODUCTION

ADVANCE manufacturing technology allows the integration of heterogeneous Intellectual Property (IP) cores on a single System-on-Chip (SoC). Commercial SoCs, such as the Intel “Xeon Phi” series [1] and Tiler “TILE-Gx” family [2], consist of SoCs up to 72 cores. Traditional bus architectures fail to scale up with the communication requirements of the increasing number of IP cores. Network-on-Chip (NoC) is the preferred communication fabric to meet the high throughput and scalability requirements between these cores. Due to time to market constraints and cost-effectiveness, SoC manufacturers tend to use third-party vendors and services from the global supply chain [3].

Typically only a few IP cores are designed in-house, while others are reusable IPs from third-party vendors. For example, FlexNoc interconnect is used by four out of the top five fabless companies to facilitate their on-chip communication [4]. A long and potentially untrusted supply chain can lead to the introduction of malicious implants through various avenues such as untrusted CAD tools, rogue designers, or at the foundry. Furthermore, these sophisticated SoC designs make it harder to do complete security verification [5]. While the design of energy-efficient NoC is the primary objective today, the security of the NoC is also crucial since exploiting NoC would be a goldmine for an attacker to access communication between various IP cores.

Figure 1 shows a 4×4 mesh NoC where mesh topology is the most commonly used topology in NoC despite the availability of many topologies. A single tile consists of

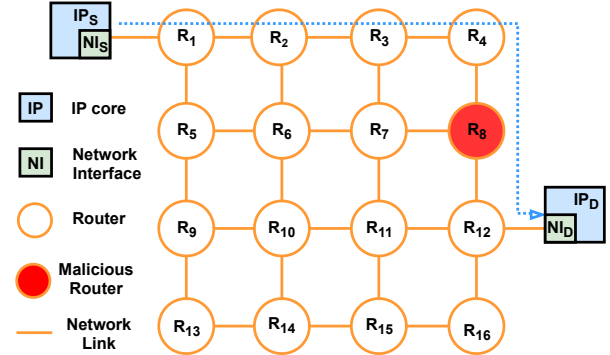


Fig. 1: NoC with 4×4 mesh topology. Each IP is connected to NoC via a network interface followed by a router. A malicious router in the middle can collect packets when IP_S communicates with IP_D .

an IP core, Network Interface (NI), and Router. Security issues in a typical NoC can be classified as eavesdropping, spoofing, denial-of-service, buffer overflow, and side-channel attacks [6]. There are efficient detection and mitigation of security vulnerabilities [6]–[10] for securing NoC-based SoCs. Anonymity ensures that there is no unauthorized disclosure of information about communicating parties. In a typical NoC, to enable fast packet forwarding, the header information is kept as plaintext while the packet data is encrypted. An adversary can implant a hardware Trojan in a router (R_8 in Figure 1), which can collect packets from the same source and launch complex cryptanalysis attacks. For example, imagine a source node (IP_S) is a cryptographic accelerator that needs to communicate with a memory controller, destination node (IP_D), to facilitate memory requests for the cryptographic operation. An adversary can use a malicious router in the middle to collect packets between IP_S and IP_D over a period of time and recover the key by launching a ciphertext-only attack. A collection of packets belonging to the same communication session also can be analyzed to discover what program is running at IP_S or reverse engineer the architectural design [11], [12]. Charles et al. [7] presented an anonymous routing solution (ArNoC) for NoC based on onion routing [13] to ensure the anonymity of a communication session.

A. Research Contributions

In this paper, we evaluate the security strength of the anonymous routing protocols in NoCs. Specifically, this paper makes the following major contributions.

- We propose an attack on existing anonymous routing by correlating NoC traffic flow using machine learning.
- We demonstrate that the proposed machine learning (ML)-based attack can break the anonymity provided by

the state-of-the-art anonymous routing (ArNoC [7]) in different configurations and traffic patterns.

- We propose a lightweight countermeasure with traffic obfuscation to defend against ML-based attacks with minor hardware and performance overhead.

The remainder of this paper is organized as follows. Section II provides relevant background and surveys the related efforts. Section III describes our ML-based attack on anonymous routing. Section IV proposes a lightweight solution that can defend against ML-based attacks. Section V presents the experimental results and evaluation. Finally, the paper is concluded in Section VI.

II. BACKGROUND AND RELATED WORK

This section provides the relevant background and surveys the related efforts to highlight the novelty of this work.

A. Network-on-Chip (NoC) Traffic

NoC enables communication by routing packets through a series of nodes. There are two types of packets that are injected into the network: control and data packets. Consider an example when a processor (IP_S) wants to load data from a particular memory controller (IP_D), it will issue a control packet requesting the data from memory. The packet will travel via routers based on a predefined routing protocol. Once the destination IP receives the control packet, it will reply with a data packet containing the requested data.

In general, header information is kept as plaintext and the payload data is encrypted. At each source NI, the packets are divided into fixed-size flits, which is the smallest unit used for flow control. There is a head flit followed by multiple body flits and tail flits. Routing in NoC can be either deterministic or adaptive; both approaches use header information to make routing decisions at each router. XY routing is the most commonly used routing in mesh-based electrical NoCs which basically takes all the X links first followed by Y links. NoC uses links to connect different components of the interconnects. Links can be either internal or boundary links. A boundary link refers to an outbound or inbound link that connects a router to a network interface, while internal links connect two routers. Our ML-based attack on anonymous routing makes use of the flow of flits (inter-flit delays), whereas, our countermeasure manipulates routing decisions to create virtual tunnels.

B. Anonymous Routing

Anonymity hides the identity of the communicating pair to anyone listening in the middle. Tor network [13] (runs on top of onion routing) and I2P network [14] (runs on top of garlic routing) are popular anonymous routing examples in traditional computer networks. Onion routing builds tunnels through a series of hops and the source applies layered encryption on the message where the number of hops equals to the number of layers, then encryption is peeled off at each hop to reveal the original message. Garlic routing is an extension of the onion routing where multiple messages are bundled and encrypted together, similar to garlic cloves. There are a wide variety of attacks to break the anonymity of the Tor network,

including flow correlation attack [15]. This attack cannot be directly applied to NoC because of the following three reasons. (i) Traffic characteristics of NoC and traditional networks are significantly different because NoC uses its traffic primarily for cache coherence messages. (ii) The existing attack relies heavily on packet size as a feature, whereas NoC flits are the fundamental unit of flow control, and they are of fixed size. (iii) All NoC nodes act as onion routers, whereas in the traditional network, there is a mixture of both normal and onion routers.

C. Related Work

Anonymity is critical for secure on-chip communication; however, the solutions in the traditional networks are too expensive for resource-constrained NoCs. Sarihi et al. [16] presented an anonymous routing that needs NoC packets to be identified as secure and non-secure packets. ARNoC [7] presented a lightweight anonymous routing protocol that considers all NoC packets. It creates an on-demand anonymous tunnel from the source to the destination where intermediate nodes know only about the preceding and succeeding nodes. Our proposed ML-based attack can break the anonymity of ARNoC.

A threat model based on the insertion of Trojans in network links is addressed in [17], [18]. Qiaoyan et al. [17] show that the Trojans can be inserted in boundary links and center links that can do bit flips in the header packet that can lead to deadlock, livelock, and packet loss. Boraten et al. [18] discuss the denial of service (DoS) attacks that can be launched by malicious links. This specific Trojan performs packet injection faults at the links which will trigger re-transmissions from the error-correcting mechanism. Frequently injecting faults will lead to multiple re-transmissions and may eventually lead to traffic hot spots in the NoC. These Trojan-based attacks are hard to detect. Our proposed attack also assumes malicious links at the points of data collection.

ML-based techniques have been used to detect and mitigate attacks on NoCs in [19]–[21]. Sudusinghe et al. [19] used several ML techniques to detect DoS attacks on NoC traffic. Reinforcement learning is used by [20] to detect hardware Trojans in NoC at run time. Sinha et al. [21] use an ML-based approach to localize flooding-based DoS attacks. None of these approaches consider attacks or countermeasures related to anonymous routing in NoC architectures. *To the best of our knowledge, our proposed ML-based flow correlation attack is the first attempt on breaking anonymity in NoC-based SoCs.*

D. Flow Correlation Challenges

NoC traffic flow can be considered a time series data array with values of increasing timestamps in order. For example, in a communication session, we can consider an array of time differences between each packet coming into a node as a flow. Flow correlation is when we take two such pairs and compare if they are correlated in some manner. For example, in a network link, the flow of inter-flit delay entering and going out of the link are correlated. Though correlating outgoing and incoming traffic on a link seems straightforward, correlating

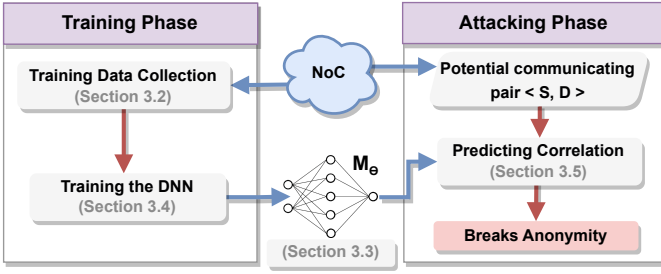


Fig. 2: Overview of our proposed ML-based attack that consists of two phases (training and attacking).

traffic between two nodes in a large network with multiple hops in NoC is extremely difficult for the following reasons:

- The queuing delay at each hop is unpredictable and can interfere with traffic flow characteristics.
- A pair of correlated nodes may communicate with other nodes, which is considered as noise.
- The communication path of the correlated pair may be shared by other nodes in SoC, which will interfere with the traffic flow characteristics between correlated pairs.

III. ML-BASED ATTACK ON ANONYMOUS ROUTING

We first outline the threat model used in the proposed attack. Next, we describe our data collection, training, and application of the ML model to accomplish the attack.

A. Threat Model

The threat model considers an NoC that uses encrypted traffic and anonymous routing using ARNoC. Therefore, when we consider an individual packet, an attacker cannot recover the payload because it's encrypted and cannot recover the sender/receiver identity because they are hidden via ARNoC. The threat model to break anonymity consists of two major components: i) a malicious NoC and ii) two malicious programs (*collector* and ML-model). The malicious NoC has malicious boundary links with Hardware Trojan (HT). The HT is capable of counting the number of cycles between flits (inter-flit-delay). Specifically, the HT can count inter-flit-delay of incoming and outgoing flits to/from an IP. After specific intervals, HT gathers all inter-flit delay into an array and sends it to the IP where the malicious program (*collector*) is running. A similar threat model of inserting HT at NoC links has been discussed in [17], [18]. Note that the area and power overhead of an HT with a small counter is insignificant in a large MPSoC [11].

The first malicious program (*collector*) runs in one of the nodes of the SoC, and it activates/deactivates HT to keep it hidden from any run-time HT detection mechanisms. The main functionality of the *collector* is to collect inter-flit-delays from HT-infected links and send them to ML-model. The second malicious program is a pre-trained ML model that runs in a remote server/cloud controlled by the adversary. The flow correlation uses the attacking phase out of two phases (attacking and training) of the ML model. The training phase is discussed in detail in Section III-D. The attacking phase is trained to classify if two inter-flit delay arrays are correlated. Figure 2 shows a high-level overview of the proposed flow correlation attack categorized from the perspective of the ML

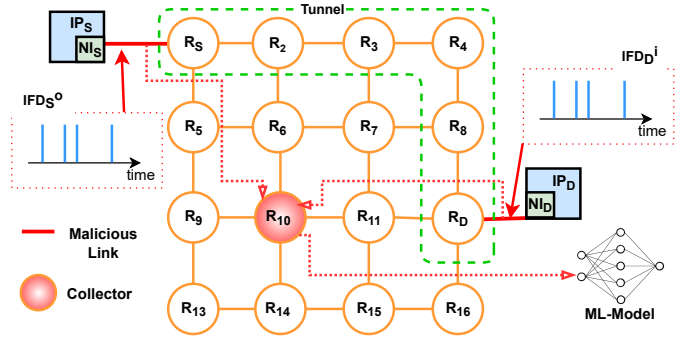


Fig. 3: Malicious boundary links outside the anonymous tunnel extract flow pair (IFD_S^o, IFD_D^i) and send them to the collector. Then, *collector* sends them to ML-model.

model. The training phase is responsible for collecting data for training and conducting training of the ML model. The training is performed before the attack, and the pre-trained model predicts the correlation of inter-flit-delays collected at runtime.

Figure 3 shows an example of the attacking phase on ARNoC. In ARNoC, a tunnel exists between source and destination routers if their associated IPs are in a communication session. ARNoC forms the tunnel to ensure anonymity by hiding the headers. The HTs in links are in the inactive state by default. The *collector* periodically checks the state of all infected boundary links and flags communicating links as suspicious. Imagine a scenario where the adversary gets suspicious of the ongoing communication between the source (IP_S) and destination (IP_D); the *collector* activates HT associated with the boundary links of IP_S and IP_D . On activation, HTs start sending periodic inter-flit delay arrays to the collector. More specifically, the Trojan will observe and leak both outbound (IFD_S^o) and inbound (IFD_D^i) traffic flows. Here, IFD_S^o refers to the outbound inter-flit delay arrays from the source IP, and IFD_D^i refers to the inbound inter-flit delay arrays at the destination IP. Upon receiving inter-flit delay arrays, the *collector* is responsible for sending collected data on inter-flit delay to the ML model. The adversary uses the ML model to pinpoint two specific nodes that are communicating and breaks the anonymity.

B. Collecting Data for Training

Algorithm 1 outlines the training data collection when running ARNoC. We collect inbound and outbound inter-flit delays for all source and destination IPs (line 4). Then, we label each flow pair as either '1' or '0' according to the ground truth (line 5). If IP_S and IP_D of flow pair $\{IFD_S^o, IFD_D^i\}$ are correlated to each other (IP_S and IP_D communicating in a session), the flow pair is tagged as '1' and otherwise '0'. These tagged flow pairs are utilized as the training set. Note that only the first l elements of each flow of flow pair $(\{IFD_S^o, IFD_D^i\})$ will be used in the training and testing. We consider the interference of external traffic (via shared path or shared resources) to correlated traffic flow characteristics by having other nodes communicating simultaneously with correlated pair communication. To evaluate the applicability of our model, we use a separate and unseen pair set during the

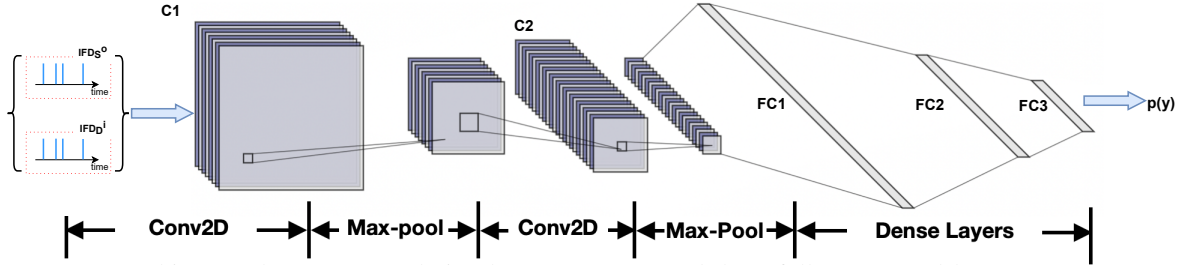


Fig. 4: DNN architecture has two convolution layers (C1, C2) and three fully connected layers (FC1, FC2, FC3).

testing phase. We utilize a deep neural network (DNN) as the ML model for our proposed flow correlation attack. In order to collect sufficient data to train DNN and make the dataset generic, we conduct multiple iterations of the data collection (Algorithm 1) by changing the mapping of correlated pairs to different NoC nodes each time. Section V elaborates on synthetic and real traffic data collection.

Algorithm 1 Data Collection

```

1:  $X, Y \leftarrow \emptyset$ 
2: procedure COLLECTDATA ()
3:   for  $\forall (s, d) \in (S, D)$  do
4:      $X \leftarrow X \cup \{ IFD_s^o, IFD_d^i \}$ 
5:      $Y \leftarrow Y \cup c : c \in \{ 0, 1 \}$ 
6:   return  $X, Y$ 

```

C. DNN Architecture

We carefully examined various configurations and reached out to the final DNN architecture shown in Figure 4. We selected Convolution Neural Networks (CNN) [22] as our model architecture for the following reasons. First, since multivariate time series have the same 2-dimensional data structures as images, CNN for analyzing images is suitable for handling multivariate time series [23]. Second, recently published works using CNN for flow correlation [15], [24] has shown promising results. Inspired by existing efforts, our final architecture has two convolution layers followed by three fully connected layers to achieve promising performance. The first convolution layer (C1) has k_1 number of kernels of size $(2, w_1)$. The second convolution layer (C2) has k_2 number of kernels of size $(2, w_2)$. The main intuition of C1 is to identify and extract the relationship between two traffic flows (IFD_s^o, IFD_d^i), while we assign the task of advancing features to C2. In our approach, both C1 and C2 have a stride of $(2, 1)$. A max-pooling layer immediately follows both convolution layers. Max pooling uses a max operation to reduce the dimension of features, which also logically reduces overfitting. Finally, the result of C2 is flattened and fed to a fully connected network with three layers. Additionally, the set (k_1, k_2, w_1, w_2) are considered as hyper-parameters. We provide details on hyper-parameter tuning in Section V-B. We use ReLU as the activation function for all convolution and fully connected layers to avoid the vanishing gradient problem and improve performance. Due to the fact that our task is a binary classification, we apply a *sigmoid* function in the last output layer to produce predictions.

D. Training the DNN Model

Algorithm 2 outlines the major steps in the training process of the ML model. Specific sizes and parameters used in training are outlined in Section V. We train the DNN for multiple epochs (line 6) for better performance of the model. We train the DNN by providing labeled inter-flit delay distributions. During the training phase, the stochastic gradient descent (*sgd*) optimizer minimizes the loss and updates the weights in the DNN (line 10). To achieve this binary classification results from the last fully connected layer pass through a *sigmoid* layer [25] (line 8) to produce classification labels.

Algorithm 2 ML Model Training

```

1:  $X : [x_1, \dots, x_j, \dots, x_N]$  where  $x_j = \{ IFD_s^o, IFD_d^i \}_j$ 
2:  $Y : [y_1, \dots, y_j, \dots, y_N]$  where  $y_j \in \{ 0, 1 \}$ 
3: procedure TRAINMODEL ( $X, Y$ )
4:   Circuit samples X and labels Y
5:   Model  $M_\Theta$  initialization
6:   for  $epoch \in [1, \dots, NoOfEpochs]$  do
7:     for  $x_j \in X$  and  $y_j \in Y$  do
8:        $out_j = \text{sigmoid}( M_\Theta(x_j) )$ 
9:        $loss = \sum_j^N \text{cross\_entropy}(out_j, y_j)$ 
10:       $\Theta = \text{sgd}(\Theta, \nabla loss)$ 
11:   Return  $M_\Theta$ 

```

Formally, the *sigmoid* layer is a normalized exponential function $f(x) = \frac{1}{1+e^{-x}}$, which aims at mapping the given vector to a probability value that lies in $[0, 1]$. The value of the output of the last layer is the predicted label $p(y)$ which can be denoted as:

$$p(y) = \frac{1}{1 + e^{-(M(s,d))}}$$

where s and d denote the source and destination input distribution respectively, and M denotes a function map for the entire DNN model.

Since it is a binary classification task, for given input (s, d) pairs' labels, their probability distributions are either $(1, 0)$ for 'true' (correlated) and $(0, 1)$ for 'false' (uncorrelated). Therefore, we choose *binary cross-entropy* (line 9) as the loss function as follows:

$$loss(p(y)) = -\frac{1}{N} \sum_{i=1}^N y_i \cdot \log(p(y_i)) + (1 - y_i) \cdot \log(1 - p(y_i))$$

where y is the label (1 for correlated pairs and 0 for uncorrelated pairs), and N is the total number of training samples.

The goal of model training is to minimize the loss function by gradient descent for multiple iterations, where in each step the model parameters Θ are updated by $\Theta' = \Theta + \nabla \text{loss}(p(y))$.

E. Predicting Correlation

The trained model can be used for automatic correlation classification. The attacking phase is simple and straightforward as shown in Algorithm 3. During the attacking phase, we feed the two inter-flit delay arrays from a suspicious source (S) and destination (D) of the ongoing communication session to the ML model (lines 4-5). The ML model will output 1 if the source and destination are communicating, and 0 otherwise (lines 5). If S and D are communicating and the ML model output is 1, our attack has successfully broken the anonymity.

Algorithm 3 Attack on Anonymous Routing

- 1: IFD_S^o : outbound inter-flit delay array of S
- 2: IFD_D^i : inbound inter-flit delay array of D
- 3: M_Θ : pre-trained model
- 4: **procedure** ATTACK ($\{IFD_S^o, IFD_D^i\}, M_\Theta$)
- 5: $p(y) \leftarrow \text{predict}(\{IFD_S^o, IFD_D^i\}, M_\Theta)$
- 6: **return** $p(y)$

IV. DEFENDING AGAINST ML-BASED ATTACKS

In this section, we propose a lightweight anonymous routing that can defend against the ML-based attack described in Section III. Figure 5 shows an overview of our proposed anonymous routing that consists of two phases: i) outbound tunnel creation and ii) data transfer with traffic obfuscation. We utilize two traffic obfuscation techniques (chaffing of flits and random delays).

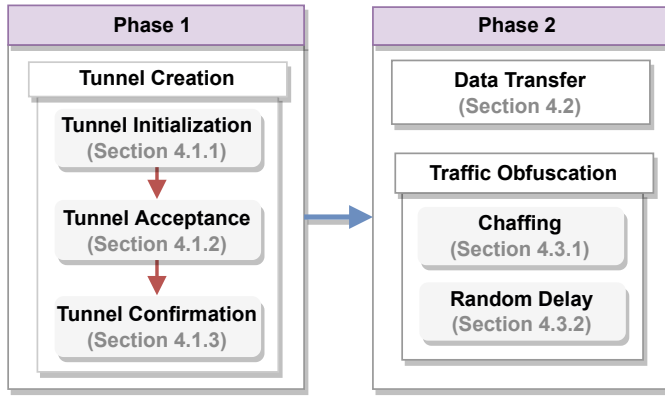


Fig. 5: Overview of the proposed lightweight anonymous routing to defend against flow correlation attack. It has two phases: tunnel creation and data transfer with traffic obfuscation.

A. Outbound Tunnel Creation

An outbound tunnel (OT_S^i) is a route created from the source router (S) of the tunnel to an arbitrary router called *tunnel endpoint* (E_S^i). Here, i indicates the parameter for each tunnel instance. Figure 6 shows how outbound tunnels, OT_S^i and OT_D^j , are used when IP_S and IP_D are injecting packets to the network. It is important to highlight that these OT^i s are only bound to their source router and are independent of

any communication session. Each tunnel is associated with a timeout bound. After the timeout, the tunnel that belongs to a particular source S will cease to exist and a new tunnel will be created with a different endpoint (E_S^{i+1}). E_S^i of an OT_S^i is randomly selected from any router that is h_{min} to h_{max} hops away from the source of the tunnel. We use $h_{min} = 3$ because a minimum of three nodes are needed for anonymous routing and increasing it further will negatively affect the performance [13]. h_{max} can be configured to balance the performance and the number of endpoint choices.

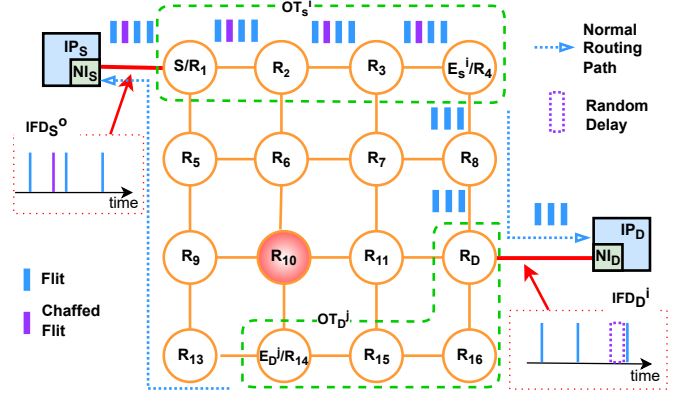


Fig. 6: Two separate outbound tunnels OT_S^i and OT_D^j are used by IP_S and IP_D for communication. In IP_S to IP_D communication, chaffed flit is inserted at NI_S and winnowed at E_S^i (R_4). E_S^i adds random delay to the flit sequence. The packet follows normal routing after an outbound tunnel ends.

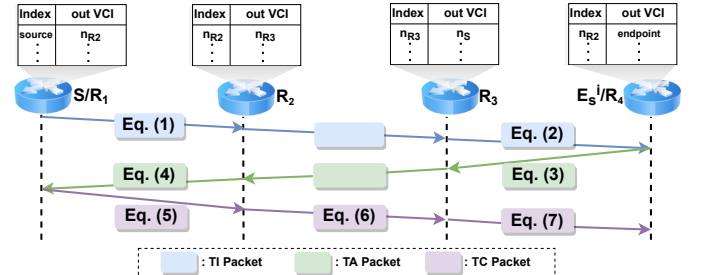


Fig. 7: Message transfer in a three-way handshake to create an outbound tunnel between router R_1 and R_4 and final state routing tables of each router representing the outbound tunnel.

Figure 7 zooms into the tunnel creation phase. A summary of notations used in tunnel creation can be found in Table I. Tunnel creation is a three-way handshake process. The source broadcasts a Tunnel Initialization (TI) packet to all the routers and only E_S^i responds back to the source with a Tunnel Acceptance (TA) packet. Once the source receives an ACK from E_S^i , it sends the Tunnel Confirmation (TC) packet to E_S^i . After these three steps, each router in the tunnel has two random Virtual Circuit Identifiers (VCI) saved in their routing table to define the succeeding and preceding hops representing the tunnel. For the rest of the section, we refer to E_S^i as just E .

1) *Tunnel Initialization*: In the example (Figure. 6), S sends a TI packet as:

$$\{TI || OPuK_S^i || E\hat{n}_{PuK_E}(OPuK_S^i || r) || TPuK_S^i\} \quad (1)$$

Algorithm 4 TI Packet handling at R

```
1:  $pkt$  : A TI packet
2: procedure HANDLETI ( $pkt$ )
3:   if  $OPuK_S^i$  in TL table then
4:     discard  $pkt$ 
5:   else
6:     store  $OPuK_S^i$  and  $TPuK_{pre(R)}^i$ 
7:   if  $D\hat{e}_{PrK_R}(pkt[3])$  is successful then
8:     GENERATETA ( $D\hat{e}_{PrK_R}(pkt[3])$ ,  $pkt[4]$ )
9:   else
10:     $pkt[4] \leftarrow TPuK_R^i$ 
11:    forward  $pkt$ 
```

TI identifies the packet as a Tunnel Initiation packet. $OPuK_S^i$ is the sources' one-time public key for the i^{th} tunnel and $OPrK_S^i$ is the corresponding private key. In other words, an OT_S^i can be uniquely identified by this key pair. PuK_E and PrK_E are the global public and private keys of E , respectively. They will not be changed with each tunnel creation. $OPuK_S^i$ and a randomly generated value r is concatenated and encrypted through public-key encryption using the key PuK_E ($E\hat{n}_{PuK_E}$). Only E can decrypt this encryption because only E has the corresponding private key (PrK_E). Finally, the temporary public key ($TPuK_S^i$) is concatenated at the end of the packet. TI packet is broadcasted instead of directly routed to avoid anonymity being broken at its birth.

Any Router (R) receiving a TI packet will follow Algorithm 4. Tunnel Lookup (TL) table has unique entries for every TI packet comes to the router. First, it tries to match $OPuK_S^i$ with the existing entries in the TL table. On match, the message will get discarded to avoid any duplication due to TI packet broadcasting (line 4). Otherwise, $OPuK_S^i$ and $TPuK_{pre(R)}^i$ are stored in the TL table (line 6). Next, R will try to decrypt the message and if it is successful, it should recognize itself as the intended endpoint and run Algorithm 5 (line 8). If not, R will replace $TPuK_{pre(R)}^i$ with its own temporary key $TPuK_R^i$ and forward the TI packet to the next hop ($next(R)$)(line 10 and 11). For example, in figure 6, after receiving a TI packet from R_2 , R_3 will generate and forward the following TI packet to R_4 :

$$\{TI||OPuK_S^i||E\hat{n}_{PuK_E}(OPuK_S^i||r)||TPuK_{R_3}^i\} \quad (2)$$

TABLE I: Notations used in tunnel creation.

$E\hat{n}_K$	Encrypts message M using key K
$D\hat{e}_K$	Decrypts message M using key K
$OPuK_S^i$	One-time public key used by source S
$OPrK_S^i$	Corresponding private key to $OPuK_S^i$
PuK_E	Global public key of E
PrK_E	Corresponding private key to PuK_E
$TPuK_R^i$	Temporary public key of node R
$TPrK_R^i$	Corresponding private key to $TPuK_R^i$
K_{S-R}	Symmetric key shared between S and R
n_R	Random nonce generated by node R
r	Random number generated by S
$pkt[i]$	i^{th} element of a packet pkt
$pre(R)$	Previous router (in upstream direction)
$next(R)$	Next router (in downstream direction)
$rand(a, b)$	Generates random number between a and b

Algorithm 5 TA packet generation at E

```
1:  $parm_1$  : parameter resolved to  $OPuK_S^i||r$ 
2: procedure GENERATETA ( $in_1$ ,  $TPuK_R$ )
3:   if  $parm_1[1] \neq OPuK_S^i$  then
4:     discard the  $pkt$ 
5:   else
6:     generate and store  $n_E$  and  $K_{S-E}$ 
7:      $enc \leftarrow E\hat{n}_{TPuK_{next(E)}^i}(E\hat{n}_{OPuK_S^i}(r||n_E||K_{S-E}))$ 
8:     return  $\{TA||enc\}$ 
```

2) *Tunnel Acceptance*: Upon receiving the TI packet, E runs Algorithm 4 first and then calls Algorithm 5 as the endpoint of the tunnel. Algorithm 5 shows the outline of TA packet generation at any endpoint router (E). First, E validates the integrity of the packet by comparing decrypted $OPuK_S^i$ value and plaintext $OPuK_S^i$ value (line 3). If the packet is validated for integrity, Algorithm 5 will execute the following steps. First, it will generate random nonce n_E which will be used as VCI. Next, it will generate a symmetric key K_{S-E} to use between S and E . Then it will log both n_E and K_{S-E} in the TL table and n_E in the *routing table* as indexed VCI (line 6). Next, it will perform encryption of the concatenation of n_E , K_{S-E} and r using the key $OPuK_S^i$ which will allow only S to decrypt the content (line 7). Finally, the resultant encryption is encrypted again by the $TPuK_{next(E)}^i$ (line 7). In the figure 6, E_S^i will generate the following TA packet:

$$\{TA||E\hat{n}_{TPuK_{R_3}^i}(E\hat{n}_{OPuK_S^i}(r||n_E||K_{S-E}))\} \quad (3)$$

When a router R receives a TA packet, it will execute Algorithm 6. If the router is the source of the OT^i , it will execute Algorithm 7 (line 4). Otherwise, it will go through the following steps. First, it decrypts the packet using the temporary private key ($TPrK_R^i$) (line 6) and generates a random nonce and symmetric key (n_R , K_{S-R}). This generated n_R and K_{S-R} are stored in R 's TL table (line 7). The nonce and symmetric key pair is concatenated to the decrypted packet (dct) (line 7 and 8), which will be encrypted using source public key ($OPuK_S^i$) to add another layer of security (line 8). Finally, R will encrypt the content with the public key of the next hop $next(R)$ (line 9). In the example, R_2 forwards the following TA packet to R_1 :

Algorithm 6 TA packet handling at R

```
1:  $pkt$  : A TA packet
2: procedure HANDLETA ( $pkt$ )
3:   if  $R$  is  $S$  of  $OT^i$  then
4:     GENERATETA ( $pkt$ )
5:   else
6:      $dct \leftarrow D\hat{e}_{TPrK_R^i}(pkt[2])$ 
7:     generate and store  $n_R$  and  $K_{S-R}$ 
8:      $enc \leftarrow E\hat{n}_{OPuK_S^i}(dct||n_R||K_{S-R})$ 
9:      $enc \leftarrow E\hat{n}_{TPuK_{next(R)}^i}(enc)$ 
10:    return  $\{TA||enc\}$ 
```

Algorithm 7 TC packet generation at S

```
1:  $pkt$  :A TA packet
2: procedure GENERATETC ( $pkt$ )
3:    $dec \leftarrow D\hat{e}_{TP_rK_S^i}(pkt[2])$ 
4:   for no of hops in OT do
5:      $dec \leftarrow D\hat{e}_{OP_rK_S^i}(dec)$ 
6:    $enc \leftarrow r$ 
7:   for R = E to next(S) do
8:      $enc \leftarrow n(R)||E\hat{n}_{K_{S-R}}(enc)$ 
9:   return  $\{TC||enc\}$ 
```

$$\{TA||E\hat{n}_{TP_uK_{R_2}^i}(E\hat{n}_{OP_uK_S^i}(E\hat{n}_{OP_uK_S^i}(E\hat{n}_{OP_uK_S^i}(r||n_E||K_{S-E})||n_{R_3}||K_{S-R_3})||n_{R_2}||K_{S-R_2}))\} \quad (4)$$

3) *Tunnel Confirmation*: Algorithm 7 depicts the TC packet generation at the source router S . $TP_rK_S^i$ is used to decrypt the outermost encryption (line 3), then each layer of the inner encryption is peeled away using the $OP_rK_S^i$ (loop from line 4 to 5). S extracts information of all the VCIs and symmetric keys. r is used to check the authenticity of the packet received (make sure the TA is a packet from the actual endpoint E). Finally, starting from E to $pre(S)$ (reverse order of routers in tunnel excluding S), r is encrypted by the respective symmetric key and concatenated with the respective nonce iteratively (loop from line 7 to 8). In the figure 6, S generates the TC packet structured as:

$$\{TC||n_{R_2}||E\hat{n}_{K_{S-R_2}}(n_{R_3}||E\hat{n}_{K_{S-R_3}}(n_E||E\hat{n}_{K_{S-E}}(r)))\} \quad (5)$$

TC denotes the packet type. The packet is layered and encrypted using the symmetric keys distributed in the previous stage. Here, n_* represents the outgoing VCI at each router from S to $prev(E)$. For example, n_{R_2} defines outgoing VCI of S and n_{R_3} defines outgoing VCI for R_2 . After the TC packet is received by each node, it decrypts the outermost layer and stores the corresponding outgoing VCI value in the routing table indexed as incoming VCI. For example, when R_2 receives the packet it will decrypt the content using key K_{S-R_2} and store the outgoing VCI as n_{R_3} in the routing table indexed as n_{R_2} . Similarly, all the routers in between S and E will update the routing table entry corresponding to the tunnel. In the example, R_2 will send TC packet to R_3 structured as follows:

$$\{TC||n_{R_3}||E\hat{n}_{K_{S-R_3}}(n_E||E\hat{n}_{K_{S-E}}(r))\} \quad (6)$$

Finally, R_3 will send the TC packet to E (R_4) structured as:

$$\{TC||(n_E||E\hat{n}_{K_{S-E}}(r))\} \quad (7)$$

B. Data Transfer

A previously created outbound tunnel (OT_S^i) is used to transfer messages anonymously from IP_S to IP_D . Before transferring the packet, the source will encrypt the actual destination header using the key K_{S-E} which is the symmetric key shared between the source and endpoint during the tunnel

creation. When we consider the data transfer through tunnel OT_S^i , a Data Transfer (DT) packet is injected into the tunnel by S structured as:

$$\{DT||n_{R_2}||E\hat{n}_{K_{S-E}}(D)||E\hat{n}_D(M)\}$$

Here, DT is the packet type identifier, n_{R_2} is the outgoing VCI, and $E\hat{n}_D(M)$ is the encrypted payload of the packet. At the router, R_2 , the outgoing VCI is identified through a simple routing table lookup on the incoming VCI of the packet. Then R_2 replaces the outgoing VCI of the packet (n_{R_2}) with the next outgoing VCI, which is n_{R_3} , and routes the packet to the next hop. Similarly, R_3 replaces the outgoing VCI of the packet to n_E . Note that any intermediate node including E does not know both source and destination of a single packet which ensures anonymity.

C. Traffic Obfuscation

We introduce traffic obfuscation techniques to hinder ML-based flow correlation. The main intuition behind the flow obfuscation is to add noise to inbound and outbound flows (IFD_S^o , IFD_D^i), so it'll be harder for ML-model to do accurate flow correlation. Section IV-C1 and IV-C2 introduce two traffic obfuscation techniques.

1) *Obfuscation with Chaffs*: We introduce a chaffing scheme as our first obfuscation technique. Chaff is a dummy flit with no usable data. Specifically, we insert chaff/chaffs in outbound tunnel traffic at the network interface of the source and filter out chaffs at the endpoint of the tunnel. The outbound flow (IFD_S^o) will have inter-flit delay data relevant to both chaffs and legitimate flits but inbound flow (IFD_D^i) will have inter-flit delay data relevant only to legitimate flits. Algorithm 8 describes the chaffing process at the NI of the source. WAKEUP procedure (Line 1 - 4) is the periodical function called by every NI in every clock cycle. We introduce a procedure named ADDCHAFF (Line 5 - 23) to obfuscate traffic through chaffing.

We insert chaffs in two specific scenarios to ensure the obfuscation scheme works with the majority of traffic patterns: (i) *first scenario*: insert chaffs in the long gap between flits (line 6 - 13), and (ii) *second scenario*: insert chaff flit in middle of closely packed flits (line 14 - 21). When the outbound link of source NI is idle for more than T_c cycles (Line 6, the first scenario is considered. The intuition behind this method is to hinder the possibility of ML-model using long inter-flit delays of inbound and outbound flows in sparse traffic scenarios. In order to control overhead, we use a percentage threshold (P_c) and ensure only P_c of idle gaps between packets get obfuscated (line 8 - 9). If chosen to be obfuscated, a dummy packet of is created and is enqueued to the output queue of the NI (line 10 - 13). At the endpoint of the tunnel, the dummy flits are filtered out and discarded. The *chaffId* header is used to identify chaffed flit or packet. In the first scenario, a hash of the NI identification number is used as chaffed id. Unlike other headers, this header is encrypted by K_{S-E} which is the symmetric key shared between the source (S) and endpoint (E) during the tunnel creation (line 12). Therefore, only endpoint can filter chaffed packets by decrypting $E\hat{n}_{K_{S-E}}(hash(NI_{ID}))$.

Algorithm 8 Add Chaff at source NI

```

1: procedure WAKEUP ( )
2:   ....
3:   ADDCHAFF(cflag)
4:   ....
5: procedure ADDCHAFF(cflag)
6:   if cflag = False and getIdleCy(linko) > Tc then
7:     cflag = True
8:     randNo  $\leftarrow$  rand(0, 99)
9:     if randNo  $\leq$  Pc then
10:      nFlits  $\leftarrow$  rand(4, 5)
11:      dPkt  $\leftarrow$  new Packet(nFlits)
12:      dPkt.chId  $\leftarrow$  E $\hat{n}_{K_{S-E}}$ (hash(NIID))
13:      outputQueue.enqueue(dummyPkt)
14:   if inputQueue.recivedPacket() = True then
15:     cflag = True
16:     randNo  $\leftarrow$  rand(0, 99)
17:     if randNo  $\leq$  Pc then
18:      chId  $\leftarrow$  rand(0, len(inputPkt))
19:      dFlit = new flit()
20:      encChId  $\leftarrow$  E $\hat{n}_{K_{S-E}}$ (hash(NIID)|chId)
21:      pkt.insert(chId, encChId, dFlit)
22:   if outputQueue.sendPacket() = True then
23:     cflag = False

```

When the input queue of source NI received a packet (line 14), the first scenario is considered (line 15 - 21). The intuition behind this scenario is to hinder the possibility of ML-model using burst of small inter flits delays of inbound and outbound flows in heavy traffic. The example shown in Figure 6 demonstrates the chaffing in second scenario and removing that chaff. Here, P_c limits the number of packets being obfuscated (line 16 - 17). If chosen to be obfuscated, chaff is inserted in the middle of legitimate packets at a random position (Line 18 - 21). K_{S-E} is used to encrypt *chaffId*, represents the position of chaff flit, which is used by the endpoint to filter the chaffed flit.

A random number generator is already in the NI for cryptographic process. Therefore, the same generator is used for random number generation in line 8, 10 and 16. If the *cflag* (line 3, 6, 7, 15 and 23) variable is true, it indicates the current gap between flits was already checked for insertion of packet. It is important to note that, (1) the dummy flits are added only when outbound link is idle, therefore, it has less impact on the program running on source IP, and (2) the dummy flits will only impact at most 3 internal links associated with the tunnel, therefore, it has less impact on the other traffic in the network. The scenario two inserts relatively less number of dummy flits and they will only impact at most 3 internal links. Experimental results in Section V-H validate that our obfuscation technique only results in negligible overhead.

2) *Obfuscation with Random Delay*: The second obfuscation technique adds random delays to selected flits and tries to tamper with the timing aspect of the traffic flow. Flits belonging to only P_d percentage of packets are subject to added delays. The tunnel endpoint is responsible for adding delays.

TABLE II: System and interconnect configuration

Parameter	Details
Processor configurations	X86, 2GHz
L1 I & D cache	1KB, 1KB (64B block size)
Coherency Protocol	MI
Topology	8×8 Mesh
Chaffing rate (P_c)	50%
Delay addition rate (P_d)	50%

Traveling through the rest of the hops the flit propagates the delay to the destination tampering with timing features of the inbound flow (IFD_D^i). Figure 6 demonstrates the effect of added delay in traffic flows. It is clear that chaffing and random delays obfuscate the actual traffic between source and destination. Both of these techniques can be used simultaneously or in a standalone manner depending on the requirement. Experimental results (Table IX and X) demonstrate that both of these techniques are beneficial in defending against ML-based flow correlation attacks.

V. EXPERIMENTAL EVALUATION

We model our proposed ML-based attack and countermeasures on a cycle-accurate Gem5 [26], a multi-core simulator, with Garnet 2.0 [27] for the interconnection network modeling. We use 64-core system with multiple and the detailed system configuration is given in Table II. Splash-2 [28] benchmark applications as well as multiple synthetic traffic patterns were used in evaluation. We used Pytorch library to implement the proposed DNN architecture. In order to evaluate the area and energy overhead of our approach against ARNoC, we implemented them in Verilog and synthesized both designs (ARNoC and our approach) using Synopsys Design Compiler with “Isi 10k” library. First, we show the results of the flow correlation attack in ARNoC [7]. Later, we show robustness of proposed countermeasure to prevent the attack.

A. Data Collection

This section demonstrates the data collection on Gem5 for the training of DNN. Although the input to DNN is in the same structure, the inherent differences in synthetic traffic and real benchmarks led us to two ways of collecting flow pairs for training.

1) *Synthetic Traffic*: We performed data collection using Uniform-Random synthetic traffic with the following modification. All IPs send packets to randomly selected IPs except two (IP_S and IP_D). These two IPs are the correlated pair communicating in a session. From all the packets injected from the source IP (IP_S), only p percent of packets are sent to the destination IP (IP_D), and the remaining packets ($(100 - p)\%$) are sent to other nodes. For example, $p = 80\%$ means 80% of the total outbound packets from IP_S will have IP_D as the destination, while the other 20% can have any other IP except IP IP_S and IP_D as the destination. Note that this 20% can be viewed as noise from the perspective of communication between IP_S and IP_D .

To make the dataset generic, for a single p value, we conduct experiments covering all possible mapping of correlated pairs to NoC nodes, which are 8064 mappings ($64 \times 63 \times 2$). We

consider four traffic distributions with p value of 95%, 90%, 85%, and 80%. In other words, we consider four different noise levels (5%, 10%, 15% and 20%) for our data collection simulations. The full dataset for a certain p value contains 24192 flow pairs ($\{IFD_S^o, IFD_D^i\}$) which consists of 8064 correlated traffic flow pairs and 16128 uncorrelated traffic flow pairs. Note that for each correlated flow pair, we selected two arbitrary uncorrelated flow pairs.

To evaluate our countermeasures, when collecting obfuscated traffic, we kept both P_c and P_d at 50% to ensure uniform distribution of obfuscation. When obfuscating traffic using added delay, we vary the delay between 1–5 cycles because a higher delay may lead to unacceptable performance overhead. We collected three categories of data sets: one with chaffing only, one with random delay only, and one with applying both chaffing and delaying simultaneously.

2) *Real Traffic*: We collected data for five Splash-2 benchmark application pairs running on two processors (P_1 and P_2) where two memory controllers (MC_1 and MC_2) are serving memory requests. The benchmark pairs used are $\{fft, fmm\}$, $\{fmm, lu\}$, $\{lu, barnes\}$, $\{barnes, radix\}$, $\{radix, fft\}$, where the first benchmark runs on P_1 and the second runs on P_2 . The selected benchmarks have the diversity to make the dataset generic (for example, fft and $radix$ are significantly different [29]). The address space of the benchmark running in P_1 is mapped only to MC_1 . Therefore, P_1 only talks with the MC_1 , and they are the correlated pair. The address space of the benchmark running in P_2 is assigned to both MC_1 and MC_2 in a way that, the ratio between memory request received by MC_1 from P_1 to memory request received by MC_1 from P_2 to be $p : (100 - p)$. This percentage p is similar to that of synthetic traffic and $(100 - p)\%$ is the noise. For example, when $p = 85\%$, MC_1 serves 15% packets to P_2 when it serves 85% packets to P_1 .

Similar to synthetic traffic, we considered four values for p which are 95%, 90%, 85%, and 80%. For a single p value and a single benchmark pair, we conducted experiments covering all possible mapping of correlated pairs to NoC nodes, which are 4032 mappings (64×63). The MC_2 and P_2 were randomly chosen in all these mappings. The full dataset for a certain p value and benchmark pair contains 16128 flow pairs (4032 correlated pairs and 12096 uncorrelated pairs). To evaluate our countermeasures, we collect obfuscated data similar to synthetic traffic.

B. Hyperparameter Tuning

Hyperparameters are the components fixed by the user before the actual training of the model begins to achieve the highest possible accuracy on the given dataset. We exhaustively tested different combinations of hyperparameters to attain state-of-the-art performance on attacking success rate. The training process consists of 10 epochs with a consistent learning rate of 0.0001. We performed batch normalization and adjusted the batch size to 10 for the training set. As for convolution layers (C1 and C2 in Figure 4), the channel size is selected as $k_1 = 1000$ and $k_2 = 2000$, with $w_1 = 5$ and $w_2 = 30$, for C1 and C2, respectively. As for fully connected

layers, sizes are selected as 3000, 800, and 100 for FC1, FC2, and FC3, respectively.

There are a lot of challenges in tuning since the finalized parameters reflect a trade-off between cost and effectiveness. First, the learning rate of the training was reduced from 0.001 to 0.0001 which increases the training time but successfully avoids the Local Minima problem. Also, we halve the training epochs from 20 to 10 to evade the Overfitting problem. Batch size is also decreased from 50 to 10. In this way, fewer samples are provided for one iteration of training, but it improves the stability of training progress. Additionally, the selection of parameters for convolution layers properly addressed their responsibilities. As discussed in Section III-C, C1 focuses on extracting rough relationships while C2 on advancing features. Therefore, C2 possesses two times of channels of C1, and a wider stride (30:5) to improve efficiency.

C. Training and Testing

In our work, a total dataset of flow pairs for a certain configuration was randomly split in a proportion of 2:1 for training and testing set. The correlated flow pairs were labeled as ‘1’ and the uncorrelated pair as ‘0’. We use the following four evaluation metrics for our experimental evaluation.

- Accuracy: $\frac{tp+tn}{tp+tn+fp+fn}$
- Recall: $\frac{tp}{tp+fn}$
- Precision: $\frac{tp}{tp+fp}$
- F1 Score: $2 \frac{Precision \cdot Recall}{Precision + Recall}$.

Here, tp , tn , fp and fn represent true positive, true negative, false positive, and false negative, respectively. Intuitively, recall is a measure of a classifier’s exactness, while precision is a measure of a classifier’s completeness, and F1 score is the harmonic mean of recall and precision. The reason for utilizing these metrics comes from the limitation of accuracy. For imbalanced test cases (e.g., $> 90\%$ positive labels), a naive ML model which gives always-true output can reach $> 90\%$ accuracy. The goal of the attacker is to identify correlating node pairs and launch complex attacks. Here, fn is when an actual correlating pair is tagged as non-correlating by the DNN. fp is when an actual non-correlating pair is tagged as correlating by the DNN. From an attacker’s perspective, the negative impact of wasting time on launching an unsuccessful attack on fp is relatively low compared to an attacker missing a chance to launch an attack due to a fn . Therefore, recall is the most critical metric compared to others when evaluating this flow correlation attack.

D. ML-based Attack on Synthetic Traffic

We evaluated the proposed attack for all four traffic distributions. The traffic injection rate was fixed to 0.01 and the IFD array size to 250. Table III summarizes the results for the attack. All the considered traffic distributions show good metric numbers. We can see a minor reduction in performance with a reducing value of p . This is expected because of the increase in the number of uncorrelated packets in correlated flow pairs, making the correlation hard to detect. Even for the lowest traffic distribution of 80% between two correlating

pairs, the attacking DNN is able to identify correlated and uncorrelated flow pairs successfully with good metric values. The slight reduction of accuracy and recall shows impact of 20% noise by other uncorrelated traffics. This confirms that our attack is realistic and can be applied on state-of-the-art anonymous routing (ARNoC) to break anonymity. More importantly, the ML model performs well in distinguishing flow correlation across different traffic characteristics with varying noise.

TABLE III: Accuracy, precision, recall and F1 score of proposed ML-based attack on existing anonymous routing (ARNoC [7]) for different traffic distributions.

p	Accuracy	Recall	Precision	F1 Score
95	97.16%	91.98%	99.47%	95.58%
90	97.04%	93.35%	97.50%	95.38%
85	94.64%	91.32%	92.30%	91.81%
80	91.70%	80.02%	94.10%	86.60%

E. Stability of ML-based Attack on Synthetic Traffic

In this section, we evaluate the attack with varying configurable parameters to further confirm the stability of the proposed ML-based attack. For experiments in this section, we use the value of p as 85% and the rest of the parameters as discussed in the experimental setup except for the varying parameter.

1) *Varying traffic injection rates (TIR)*: We collected traffic data for four traffic injection rates: 0.001, 0.005, 0.01 and 0.05, and conducted the attack on existing anonymous routing. Table IV provides detailed results on metrics over selected values. We can see a small reduction in overall metrics including recall, with the increase in injection rate. This is because, higher injection rates will create more congestion and buffering delays on NoC traffic. The indirect noise from congestion and buffering delays makes it slightly hard for the ML model to do flow correlation. Overall, our proposed ML model performs well in different injection rates since all the metrics show good performance.

TABLE IV: Accuracy, precision, recall and F1 score of proposed ML-based attack on existing anonymous routing for different traffic injection rates.

TIR	Accuracy	Recall	Precision	F1 Score
0.001	95.32%	92.29%	93.51%	92.89%
0.005	94.72%	90.14%	93.98%	92.02%
0.01	94.64%	91.32%	92.30%	91.81%
0.05	93.86%	88.56%	92.67%	90.56%

2) *Varying IFD Array Size*: We collected traffic data by varying the size of IFD array size (l) in the range of 50 to 550 and conducted the attack on existing anonymous routing. Table V shows detailed results on metrics over selected values. For a lower number of flits, the relative values of the recall and other metrics are low. However, with the increasing number of flits, the accuracy also improves until the length is 250. This is due to the increase in the length of the IFD array the ML model has more features for the flow correlation. After the value of 250, the accuracy saturates at around 94.5%. In subsequent experiments, we kept l to 250 because ML-based attack performs relatively well with less monitoring time.

TABLE V: Proposed ML-based attack on existing anonymous routing for varying number of flits.

IFD Array size(l)	Accuracy	Recall	Precision	F1 Score
50	83.53%	96.45%	67.96%	79.74%
100	90.92%	96.17%	80.28%	87.51%
150	90.93%	74.10%	98.32%	84.51%
250	94.64%	91.32%	92.30%	91.81%
350	94.71%	86.21%	97.39%	91.46%
450	94.58%	93.21%	90.58%	91.87%
550	94.66%	88.97%	94.30%	91.56%

3) *Varying Network Size*: To evaluate the stability of the ML model on varying network sizes, we analyzed the model on 16 core system with 4×4 , 64 core system with 8×8 , and 256 core system with 16×16 mesh topology. Table VI shows the performance results of the ML model for different network sizes. Attack on 4×4 mesh shows slightly good metric values compared to 8×8 . Attack on 16×16 shows relatively low accuracy and recall since a large network tends to alter temporal features of the traffic due to increased congestion and number of hops. Considering good accuracy and other metrics, our ML-based attack shows stability across different mesh sizes.

TABLE VI: Proposed ML-based attack on existing anonymous routing for different mesh sizes.

Mesh Size	Accuracy	Recall	Precision	F1 Score
4×4	94.76%	91.86%	92.63%	92.24%
8×8	94.64%	91.32%	92.30%	91.81%
16×16	92.72%	80.28%	96.98%	87.84%

F. ML-based Attack on Real Benchmarks

We trained and tested the model using two techniques. In the first technique, we merge datasets of a single p value across all 5 benchmark combinations outlined in Section V-A to create the total dataset. Therefore, the total dataset has 80640 flow pairs before the 2:1 test to train split. Table VII summarizes the results for the first technique across all p values. Good metric numbers across all traffic distributions show the generality of the model across different benchmarks. In other words, our attack works well across multiple benchmarks simultaneously. Even 20% noise ($p = 80$) shows recall value just below 99% making the attack more favorable to an attacker as discussed in Section V-C. We can see a minor reduction of performance with reduction in p , which is expected due to increased noise in the correlated flow pair.

TABLE VII: Accuracy, precision, recall and F1 score of proposed ML-based attack on ARNoC [7] for different noise levels for real benchmarks.

p	Accuracy	Recall	Precision	F1 Score
95	99.43%	99.79%	98.01%	98.89%
90	99.11%	99.84%	96.75%	98.27%
85	98.76%	98.16%	97.01%	97.58%
80	96.08%	98.79%	87.15%	92.61%

When we compare the performance of attack on real traffic against synthetic traffic (Table III), attack on real traffic shows better performance. This is primarily for two reasons. (a) The synthetic traffic generation is totally random. More precisely,

the interval between two packets is random and the next destination of a specific source is random. This level of randomness is not found in real traffic making flow correlation in real traffic relatively easy. (b) In synthetic traffic all 64 nodes talk with each other making higher buffering delays eventually making flow correlation harder. However, buffering delays has minor impact compared to randomness.

The second technique use dataset of a single p value and single benchmark pair. Table VII summarizes the results for the second technique when $p = 85$ across five benchmark pairs. All benchmarks shows good metric values, but we can see slight reduction of accuracy and average recall in 3rd and 4th rows. Both benchmark pairs have *barnes* benchmark, which has lowest bytes per instruction in all benchmarks [30]. This results in sparse inter-flit array, eventually making it relatively harder to do flow correlation.

TABLE VIII: Accuracy, precision, recall and F1 score of our ML-based attack on existing anonymous routing (ARNoC [7]) when $p=85$ across real benchmarks.

benchmark	Accuracy	Recall	Precision	F1 Score
{fft, fmm}	98.29%	99.11%	94.42%	96.71%
{fmm, lu}	99.32%	97.63%	99.70%	98.65%
{lu, barnes}	97.84%	91.60%	99.76%	95.51%
{barnes, radix}	96.14%	84.59%	99.73%	91.54%
{radix, fft}	96.62%	97.05%	90.66%	93.75%

G. Robustness of the Proposed Countermeasure

We discuss the robustness of our proposed lightweight anonymous routing in two ways. First, we discuss the robustness of our proposed countermeasure (Section IV) against the ML-based attack (Section III) on both synthetic and real traffic. Second, we discuss the robustness of our proposed attack in terms of breaking anonymity in general.

We evaluate our countermeasure against ML-based attack in three configurations for synthetic traffic: (i) using chaffing, (ii) using a delay, and (iii) using both chaffing and delay to obfuscate traffic. For each of the three configurations, we evaluate the ML-based attack on two scenarios: (1) train with non-obfuscated traffic and test with obfuscated traffic (Table IX), and (2) train and test with obfuscated traffic (Table X). In all three configurations, the attack on the first scenario has performed poorly (the proposed countermeasure defends very well). This is expected because the attacking DNN has not seen any obfuscated data in the training phase. If we focus on the scenario of using a delay to obfuscate traffic (Table X), we can see a significant reduction in all the metrics. Large drops in recall when using chaffing as the obfuscation technique validate that the proposed countermeasure produces a significant negative impact on attackers' end goals. Adding random delay reduces accuracy and recall by about 3% compared to non-obfuscated traffic in all the traffic distributions. Whereas, combining chaffing with delay reduces accuracy and recall by about 3% as compared to chaffing alone. In other words, combining two obfuscation techniques did not seem to have any synergistic effect. We recommend chaffing as a good obfuscation configuration since adding delay has only a small advantage despite its overhead. Note that the poor performance

of added random delay as a countermeasure validates the fact that our proposed attack is robust against inherent random network delays in the SoC.

When evaluating the performance of countermeasures using benchmark applications, we consider only chaffing to obfuscate traffic. Furthermore, we only train and test with obfuscated traffic which guarantees to give a strong evaluation of the countermeasure. As discussed in section V-F we evaluate the countermeasure using two techniques, (i) merged datasets across benchmarks (Table XI) and (ii) datasets per benchmark when p value is fixed (Table XII). When we focus on Table XI, we see an overall reduction of metric values compared to the attack without countermeasure. Even though the accuracy reduction is around 10%, the countermeasure has reduced recall value drastically. This will negatively affect the attacker due to missing a chance to launch an attack due to higher fn . When we compare the performance of the countermeasure on real traffic against synthetic traffic (Table X), the countermeasure on synthetic traffic has performed relatively better. This is due to the same two reasons mentioned in section V-F briefly, the randomness of synthetic traffic and increased buffer delay because every node communicates.

We evaluate the anonymity of proposed lightweight anonymous routing in three attacking scenarios. The first scenario is when *one of the intermediate routers in the outbound tunnel is malicious*. The malicious router only knows the identity of the preceding and succeeding router, so the anonymity of the flits traveling through the tunnel is secured. The second scenario is when *the tunnel endpoint is malicious*. The router will have the actual destination of the packet but not the source information; therefore by having a single packet, the malicious router cannot break the anonymity. This scenario is also considered secure in the traditional onion routing threat model [13]. Complex attacks in malicious routers need a considerable number of packets/flits to be collected. It is hard due to two following reasons: (i) Our proposed solution changes the outbound tunnel of a particular source frequently. (ii) Since the source and destination have two independent outbound tunnels, it is infeasible to collect and map request/reply packets. The final scenario is when *an intermediate router in a normal routing path is malicious*. This scenario arises when flits use normal routing after it comes out of the outbound tunnel. Similar to the previous scenario, the packet only knows about the true destination, and anonymity is not broken using a single packet. In other words, outbound tunnels change frequently, and the source and destination have different tunnels making it hard to launch complex attacks to break anonymity by collecting packets.

We evaluate the robustness of our approach in terms of deadlock handling. We have implemented our model using Garnet 2.0, where the XY routing mechanism is used to guarantee deadlock-free communication. When we focus on our countermeasure, the outbound tunnel forces packets to disregard XY routing protocol. So, the introduction of an outbound tunnel can have the potential to create a deadlock. The first step of tunnel creation (Tunnel Initialization) uses the existing XY routing protocol to broadcast TI packets. The path of the TI packet determines the tunnel shape. Since a TI packet

TABLE IX: Accuracy, precision, recall and F1 score of ML-based attack on proposed lightweight anonymous routing for different traffic distributions when trained with non-obfuscated traffic and tested with obfuscated traffic

p	Chaffing				Delay				Chaffing + Delay			
	Acc.	Rec.	Prec.	F1.	Acc.	Rec.	Prec.	F1.	Acc.	Rec.	Prec.	F1.
95	66.55%	0.3%	33.33%	0.6%	81.32%	56.70%	81.67%	66.93%	63.36%	14.37%	37.18%	20.70%
90	66.59%	25.68%	49.78%	33.88%	71.73%	66.15%	56.48%	60.94%	56.47%	42.27%	40.45%	41.34%
85	61.2%	2.6%	12.4%	4.4%	72.57%	50.59%	60.61%	55.15%	66.33%	40.50%	49.39%	44.51%
80	72.76%	26%	77.16%	38.89%	73.41%	34.97%	70.37%	46.72%	60.34%	30.72%	39.75%	34.65%

TABLE X: Accuracy, precision, recall and F1 score of ML-based attack on proposed lightweight anonymous routing for different traffic distributions when trained and tested with non-obfuscated traffic

p	Chaffing				Delay				Chaffing + Delay			
	Acc.	Rec.	Prec.	F1.	Acc.	Rec.	Prec.	F1.	Acc.	Rec.	Prec.	F1.
95	76.64%	33.60%	84.67%	48.11%	94.22%	87.31%	94.99%	90.99%	73.80%	25.49%	80.70%	38.75%
90	79.45%	43.71%	87.39%	58.28%	93.58%	93.42%	87.66%	90.45%	77.95%	46.9%	78.14%	58.69%
85	78.75%	38.93%	93.16%	54.92%	90.65%	86.83%	84.99%	85.90%	77.06%	48.85%	74.65%	59.05%
80	79.75%	74.41%	67.58%	70.83%	87.70%	80.32%	82.08%	81.19%	77.56%	74.41%	64.13%	68.89%

TABLE XI: Accuracy, precision, recall and F1 score of ML-based attack on proposed lightweight anonymous routing different noise levels for real benchmarks.

p	Accuracy	Recall	Precision	F1 Score
95	89.93%	76.67%	82.44%	79.45%
90	88.78%	77.08%	78.30%	77.69%
85	87.63%	62.04%	84.34%	71.49%
80	85.89%	76.85%	70.23%	73.39%

TABLE XII: Accuracy, precision, recall and F1 score of ML-based attack on proposed lightweight anonymous routing for real benchmarks.

benchmark	Accuracy	Recall	Precision	F1 Score
{ft, fmm}	87.64%	65.91%	80.24%	72.37%
{fmm, lu}	90.67%	83.03%	80.20%	81.59%
{lu, barnes}	84.98%	57.75%	76.19%	65.70%
{barnes, radix}	84.24%	40.35%	97.59%	57.10%
{radix, fft}	82.60%	37.67%	82.66%	51.79%

cannot take a Y to X turn, any tunnel created on XY routing inherently use only XY turns inside the tunnel. Hence in the data transfer phase, all the communication inside and outside the outbound tunnel will only take X to Y turns, ensuring deadlock-free communication.

H. Overhead of the Proposed Countermeasure

Figure 8a shows the average packet latency for our proposed lightweight countermeasure over ARNoC in the data transmission phase. Obfuscating with chaff flit, which is the recommended obfuscation technique from Section V-G has only a 13% increase in performance overhead. When we consider tunnel creation overhead in Figure 8b, our approach performs 35.53% better compared to ARNoC. The most important aspect to highlight is that in our approach tunnel creation can happen in the background. Therefore, our tunnel creation does not directly affect the data transfer performance. Overall, our approach is lightweight compared to ARNoC while delivering anonymity against ML-based attacks.

In addition to low performance overhead, our lightweight anonymous routing has the inherent advantage of utilizing any adaptive routing mechanisms supported by NoC architectures (endpoint of output tunnel to the destination), while ARNoC

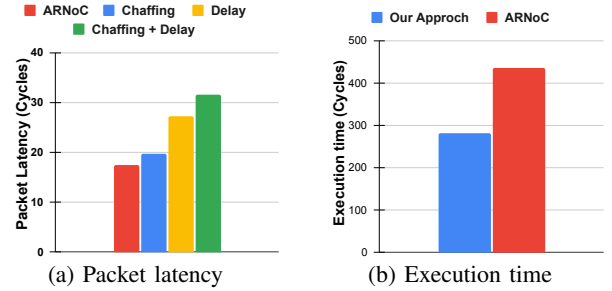


Fig. 8: Comparison of proposed countermeasure versus ARNoC: (a) average packet latency of data transfer phase and (b) average execution time for tunnel creation phase.

cannot accommodate adaptive routing protocols because of having a pre-built tunnel from the source to destination.

TABLE XIII: Comparison of the area and power overhead between ARNoC and proposed countermeasure in NoC IP.

	ARNoC	Our Approach	Overhead
Area	1710665	1741257	+ 1.7%
Power(mW)	1607.40	1617.51	+ 0.6%

Table XIII compares the area and power overhead of our lightweight countermeasure against ARNoC in 8×8 mesh topology. In the implementation, our approach uses only the chaffing obfuscation. There is only a 1.7% increase in area and only a 0.6% increase in power. The area and power overhead are negligible considering the performance improvement and additional security provided by our proposed anonymous routing compared to the state-of-the-art anonymous routing ARNoC [7].

VI. CONCLUSION

Network-on-Chip (NoC) is a widely used solution for on-chip communication between Intellectual Property (IP) cores in System-on-Chip (SoC) architectures. Anonymity is a critical requirement for designing secure and trustworthy NoCs. In this paper, we made two important contributions. We proposed a machine learning-based attack that uses traffic correlation to break the state-of-the-art anonymous routing for NoC architectures. We developed a lightweight and robust anonymous routing protocol to defend against ML-based attacks. Extensive evaluation using real as well as synthetic traffic demonstrated

that our ML-based attack can break anonymity with high accuracy (up to 99%) for diverse traffic patterns. The results also reveal that our lightweight countermeasure of obfuscating traffic with chaffing is robust against ML-based attacks with minor hardware overhead. The performance overhead of our proposed countermeasure is significantly less compared to the state-of-the-art anonymous routing protocol for NoC-based SoCs.

ACKNOWLEDGMENTS

This work was partially supported by National Science Foundation (NSF) grant SaTC-1936040.

REFERENCES

- [1] G. Chrysos, "Intel® xeon phi™ coprocessor-the architecture," *Intel Whitepaper*, vol. 176, p. 43, 2014.
- [2] C. Ramey, "Tile-gx100 manycore processor: Acceleration interfaces and architecture," in *2011 IEEE Hot Chips 23 Symposium (HCS)*. IEEE, 2011, pp. 1–21.
- [3] P. Mishra *et al.*, *Network-on-Chip Security and Privacy*. Springer Nature, 2021.
- [4] R. JS *et al.*, "Runtime detection of a bandwidth denial attack from a rogue network-on-chip," in *Proceedings of the 9th International Symposium on Networks-on-Chip*. ACM, 2015, p. 8.
- [5] P. Mishra, S. Bhunia, and M. Tehranipoor, *Hardware IP security and trust*. Springer, 2017.
- [6] S. Charles *et al.*, "A survey of network-on-chip security attacks and countermeasures," *ACM Computing Surveys (CSUR)*, vol. 54, no. 5, pp. 1–36, 2021.
- [7] S. Charles *et al.*, "Lightweight Anonymous Routing in NoC based SoCs," in *Design Automation & Test in Europe (DATE)*, 2020.
- [8] F. Farahmandi *et al.*, *System-on-Chip Security: Validation and Verification*. Springer Nature, 2019.
- [9] Y. Lyu *et al.*, "Scalable activation of rare triggers in hardware trojans by repeated maximal clique sampling," *IEEE Transactions on Computer-Aided Design of Integrated Circuits and Systems*, 2020.
- [10] A. Ahmed *et al.*, "Scalable hardware trojan activation by interleaving concrete simulation and symbolic execution," in *2018 IEEE International Test Conference (ITC)*. IEEE, 2018, pp. 1–10.
- [11] M. M. Ahmed, A. Dhavle, N. Mansoor, P. Sutradhar, S. M. P. Dinakarrao, K. Basu, and A. Ganguly, "Defense against on-chip trojans enabling traffic analysis attacks," in *2020 Asian Hardware Oriented Security and Trust Symposium (AsianHOST)*. IEEE, 2020, pp. 1–6.
- [12] M. M. Ahmed, A. Dhavle, N. Mansoor, S. M. P. Dinakarrao, K. Basu, and A. Ganguly, "What can a remote access hardware trojan do to a network-on-chip?" in *2021 IEEE International Symposium on Circuits and Systems (ISCAS)*. IEEE, 2021, pp. 1–5.
- [13] R. Dingleline *et al.*, "Tor: The second-generation onion router," Naval Research Lab Washington DC, Tech. Rep., 2004.
- [14] B. Zantout, R. Haraty *et al.*, "I2p data communication system," in *Proceedings of ICN*. Citeseer, 2011, pp. 401–409.
- [15] M. Nasr *et al.*, "Deepcorr: Strong flow correlation attacks on tor using deep learning," in *Proceedings of the 2018 ACM SIGSAC Conference on Computer and Communications Security*, 2018, pp. 1962–1976.
- [16] A. Sarihi *et al.*, "Securing network-on-chips via novel anonymous routing," in *Proceedings of the 15th IEEE/ACM International Symposium on Networks-on-Chip*, 2021.
- [17] Q. Yu *et al.*, "Exploiting error control approaches for hardware trojans on network-on-chip links," in *International symposium on defect and fault tolerance in VLSI and nanotechnology systems (DFTS)*, 2013, pp. 266–271.
- [18] T. Boraten *et al.*, "Mitigation of denial of service attack with hardware trojans in noc architectures," in *Parallel and Distributed Processing Symposium, 2016 IEEE International*. IEEE, 2016, pp. 1091–1100.
- [19] C. Sudusinghe *et al.*, "Denial-of-service attack detection using machine learning in network-on-chip architectures," in *Proceedings of the 15th IEEE/ACM International Symposium on Networks-on-Chip*, 2021, pp. 35–40.
- [20] K. Wang *et al.*, "Tsa-noc: Learning-based threat detection and mitigation for secure network-on-chip architecture," *IEEE Micro*, vol. 40, no. 5, pp. 56–63, 2020.
- [21] M. Sinha *et al.*, "Sniffer: A machine learning approach for dos attack localization in noc-based socs," *IEEE Journal on Emerging and Selected Topics in Circuits and Systems*, 2021.
- [22] J. Schmidhuber, "Deep learning in neural networks: An overview," *Neural networks*, vol. 61, pp. 85–117, 2015.
- [23] B. Zhao *et al.*, "Convolutional neural networks for time series classification," *Journal of Systems Engineering and Electronics*, vol. 28, no. 1, pp. 162–169, 2017.
- [24] S. Guo, Y. Lin, S. Li, Z. Chen, and H. Wan, "Deep spatial-temporal 3d convolutional neural networks for traffic data forecasting," *IEEE Transactions on Intelligent Transportation Systems*, vol. 20, no. 10, pp. 3913–3926, 2019.
- [25] J. Han and C. Moraga, "The influence of the sigmoid function parameters on the speed of backpropagation learning," in *From Natural to Artificial Neural Computation: International Workshop on Artificial Neural Networks Malaga-Torremolinos, Spain, June 7–9, 1995 Proceedings 3*. Springer, 1995, pp. 195–201.
- [26] N. Binkert *et al.*, "The gem5 simulator," *SIGARCH Computer Architecture News*, 2011.
- [27] N. Agarwal *et al.*, "GARNET: A detailed on-chip network model inside a full-system simulator," *ISPASS*, 2009.
- [28] C. Sakalis, S. Leonardsson, S. Kaxiras, and A. Ros, "Splash-3: A properly synchronized benchmark suite for contemporary research," in *2016 IEEE International Symposium on Performance Analysis of Systems and Software (ISPASS)*. IEEE, 2016, pp. 101–111.
- [29] C. Bienia, S. Kumar, and K. Li, "Parsec vs. splash-2: A quantitative comparison of two multithreaded benchmark suites on chip-multiprocessors," in *2008 IEEE International Symposium on Workload Characterization*. IEEE, 2008, pp. 47–56.
- [30] S. C. Woo, M. Ohara, E. Torrie, J. P. Singh, and A. Gupta, "The splash-2 programs: Characterization and methodological considerations," *ACM SIGARCH computer architecture news*, vol. 23, no. 2, pp. 24–36, 1995.

Hansika Weerasena is a Ph.D student in the Department of Computer & Information Science & Engineering at the University of Florida. He received his BSc in Department of Computer Science and Engineering from university of Moratuwa, Sri Lanka. His area of research includes cyber and hardware communication security, computer architecture and machine learning.



Zhixin Pan is a Ph.D student in the Department of Computer & Information Science & Engineering at the University of Florida. He received his B.E. in the Department of Software Engineering from Huazhong University of Science & Technology, Wuhan, China in 2015. His area of research includes cyber & hardware Security, post-silicon debug, data mining and machine learning.



Khushboo Rani is a Postdoctoral associate in the Department of Computer & Information Science & Engineering at the University of Florida. She received her Ph.D. in Computer Science and Engineering from the Indian Institute of Technology Guwahati, India in 2021. Her area of research includes network-on-chip, systems-on-chip, memory system design, embedded systems, side-channel analysis, hardware security and trust, and malware detection.



Prabhat Mishra is a Professor in the Department of Computer and Information Science and Engineering at the University of Florida. He received his Ph.D. in Computer Science from the University of California at Irvine in 2004. His research interests include embedded and cyber-physical systems, hardware security and trust, and energy-aware computing. He currently serves as an Associate Editor of IEEE Transactions on VLSI Systems and ACM Transactions on Embedded Computing Systems. He is an IEEE Fellow and an ACM Distinguished Scientist.

